STRONG EVIDENCE AGAINST A NON-DEGENERATE COMPANION IN SN 2012CG

B. J. SHAPPEE[1,2], A. L. PIRO[1], K. Z. STANEK[3,4], S. G. PATEL[1], R. A. MARGUTTI[5,6], V. M. LIPUNOV[7,8], AND R. W. POGGE[3,4]

(Dated: October 26, 2016)
Draft version October 26, 2016

ABSTRACT

Even though SN 2012cg is one of the best-studied Type Ia Supernovae to date, the nature of its progenitor system has been debated in numerous studies. Specifically, it is difficult to reconcile the claims of the detection of a $\sim 6\,M_\odot$ main-sequence companion by Marion et al. (2016) with the deep, late-time Hα flux limits from Maguire et al. (2016). In this study we add three new constraints: 1) We analyze a high-signal-to-noise, nebular-phase, LBT/MODS spectrum of SN 2012cg and place an upper limit on the amount of low-velocity, solar-abundance material removed from a possible companion of $< 7.8 \times 10^{-3}\,M_\odot$. 2) We use *Swift* X-ray observations to constrain the preexplosion mass-loss rate to be $\dot{M} < 10^{-6}\,M_\odot\,\mathrm{yr}^{-1}$ for $v_\mathrm{w} = 100\,\mathrm{km\,s}^{-1}$. 3) We carefully reanalyze a prediscovery MASTER image and, with published light curves of SN 2012cg, we estimate the time of first light and conservatively constrain the radius of a Roche-lobe overflowing companion to be $< 0.23\,R_\odot$. These observations strongly disagree with Marion et al. (2016), and, when considered with other studies of SN 2012cg's progenitor system, essentially rule out a non-degenerate companion.

Subject headings: supernovae: specific (SN 2012cg)

1. INTRODUCTION

The physical nature of the progenitor systems of Type Ia Supernovae (SNe Ia) remains largely elusive despite decades of work (for a review see Wang & Han 2012). It is generally accepted that SNe Ia result from the thermonuclear explosion of a carbon-oxygen white dwarf (WD; Hoyle & Fowler 1960) in a close binary system, but there are still two competing classes of models. In the double-degenerate (DD) model, the WD's companion is another WD where the binary merges either due to the removal of energy and angular momentum from the system by gravitational radiation (Tutukov & Yungelson 1979; Iben & Tutukov 1984; Webbink 1984) or due to the perturbations of a third (e.g., Thompson 2011; Katz & Dong 2012; Shappee & Thompson 2013; Antognini et al. 2014) or fourth (Pejcha et al. 2013) body. In the single-degenerate (SD) model, the WD's companion is a non-degenerate star (Whelan & Iben 1973; Nomoto 1982). In most current models, the WD accretes matter from the non-degenerate companion until the WD undergoes unstable runaway nuclear burning. However, many current explosion simulations of both SD (e.g. Kasen et al. 2009) and DD (e.g. Pakmor et al. 2012) progenitors can match the observable signatures of SNe Ia around B-band maximum light ($t_{B\mathrm{max}}$), and observational searches for distinguishing characteristics be-

tween these two models have proven difficult.

Despite these challenges, significant progress has been made during the past decade, and some classes of SD models have been observationally ruled out as the dominant channel (e.g., Bianco et al. 2011; Lipunov et al. 2011; Chomiuk et al. 2016; Maguire et al. 2016). However, there are still candidate SD progenitor systems (e.g. U Sco and V445 Pup; Li et al. 2011). Additionally, in the past few years, detailed studies of individual nearby SNe Ia have proven particularly fruitful. A prime example is SN 2011fe, the brightest SN Ia in almost 40 years at just 6.4 Mpc away (Shappee & Stanek 2011), which was discovered by the Palomar Transient Factory (PTF; Law et al. 2009) less than one day after explosion. For SN 2011fe, none of the observational signatures expected for SD channels have been seen (Nugent et al. 2011; Horesh et al. 2012; Chomiuk et al. 2012b; Margutti et al. 2012; Brown et al. 2012; Shappee et al. 2013b), while early-light-curve properties (Piro et al. 2010; Bloom et al. 2012) and direct evidence for nuclear synthetic yields argue for a DD channel (Shappee et al. 2016a). However, there might be multiple channels for producing normal SNe Ia (e.g., Maguire et al. 2013; Yamaguchi et al. 2015), so additional well-studied SNe Ia are needed.

In the SD model, the companion is expected to be struck by the SN ejecta soon after explosion. This feature of the SD model has proven to be a fruitful observational test. First, the interaction of the SN ejecta with the companion will modify the rising light curve at early times. Such a signature is dependent on the viewing angle, and the strongest effect will occur when the companion lies along the line of sight between the observer and the SN. At a fixed viewing angle, this emission scales proportionally with the companion's radius (R_c), which allows early-time observations to constrain the properties of the companion (Kasen 2010). Second, material from the companion will be stripped when struck by the SN ejecta (e.g., Wheeler et al. 1975; Marietta et al. 2000; Meng et al. 2007; Pakmor et al. 2008; Pan et al. 2012b; Liu et al. 2012). Pan et al. (2012b) and Liu et al. (2012) use hydrodynamic simulations to show that $\sim 0.1 - 0.2\,M_\odot$ of solar-metallicity material is expected to be removed from main-sequence (MS)

bshappee@obs.carnegiescience.edu

[1] Carnegie Observatories, 813 Santa Barbara Street, Pasadena, CA 91101, USA

[2] Hubble, Carnegie-Princeton Fellow

[3] Department of Astronomy, The Ohio State University, 140 West 18th Avenue, Columbus, OH 43210, USA

[4] Center for Cosmology and AstroParticle Physics (CCAPP), The Ohio State University, 191 W. Woodruff Ave., Columbus, OH 43210, USA

[5] Center for Interdisciplinary Exploration and Research in Astrophysics (CIERA) and Department of Physics and Astronomy, Northwestern University, Evanston, IL 60208, USA

[6] Center for Cosmology and Particle Physics, New York University, 4 Washington Place, New York, NY 10003, USA

[7] M.V.Lomonosov Moscow State University, Physics Department, Leninskie gory, GSP-1, Moscow, 119991, Russia

[8] M.V.Lomonosov Moscow State University, Sternberg Astronomical Institute, Universitetsky pr., 13, Moscow, 119234, Russia

companions and that this material will be embedded in low-velocity supernova debris with a characteristic velocity of $\lesssim 1000$ km s^{-1}. Initially, this material will be hidden by the higher-velocity, optically thick, iron-rich ejecta, but will then appear in late-time, nebular-phase spectra ($\gtrsim 250$ days; Mattila et al. 2005) as the higher-velocity ejecta become optically thin. Finally, this impact is expected to affect the companion's future properties (Podsiadlowski 2003; Pan et al. 2012a; Shappee et al. 2013a).

The Lick Observatory Supernova Search (LOSS; Filippenko et al. 2001) discovered the nearby SN 2012cg in NGC 4424 ($z = 0.001458 + \pm 0.000007$; Kent et al. 2008) on 2012 May 17.2 UT (MJD = 56064.22) and quickly announced it to the community (Cenko et al. 2012). Munari et al. (2013) determined $t_{B\rm max}$ was 2012 June 4.5 UT (MJD=56082.0). At just 15.2 ± 1.9 Mpc ($\mu = 30.90 \pm 0.3$ mag; Cortés et al. 2008), SN 2012cg has been an ideal candidate for extensive follow-up with multiwavelength studies in the radio (Chomiuk et al. 2012a, 2016), the far-infrared (far-IR) with Herschel (Johansson et al. 2013), the IR with the Hubble Space Telescope (HST; Amanullah et al. 2015), the optical from the ground (Silverman et al. 2012; Munari et al. 2013; Yamanaka et al. 2014; Amanullah et al. 2015; Maguire et al. 2016; Marion et al. 2016) and HST (Amanullah et al. 2015; Graur et al. 2016), the ultraviolet (UV) with *Swift* (Marion et al. 2016) and HST (Amanullah et al. 2015), and X-rays with *Swift* (Margutti & Soderberg 2012).

However, even though SN 2012cg is one of the best-studied SNe Ia to date, the nature of its progenitor remains debated in a number of studies:

(1) Silverman et al. (2012) claim that their early-time observations from the 0.76m Katzman Automatic Imaging Telescope (KAIT) rule out a ~ 1 M$_\odot$ ($a \approx 2$ R$_\odot$) main-sequence companion for certain viewing angles and red-giant companions ($a \approx 400$ R$_\odot$) for almost all viewing angles.

(2) Marion et al. (2016) use the same KAIT observations with additional observations from the F. L. Whipple Observatory 1.2m (FLWO), the Las Cumbres Observatory Global Telescope Network (LCOGT; Brown et al. 2013), *Swift*, and ROTSE-IIIb (Akerlof et al. 2003) to argue that they see a blue, early-time excess in the optical light curve consistent with the Kasen (2010) models of the SN ejecta interacting with a ~ 6 M$_\odot$ main-sequence companion.

(3) Chomiuk et al. (2012a, 2016) observed SN 2012cg with the Karl G. Jansky Very Large Array to place some of the deepest radio limits of any SNe Ia.[9] The resulting limits on any preexisting wind are inconsistent with those observed for symbiotic binaries and most isolated red giants (Chomiuk et al. 2016). Main-sequence B stars with $\gtrsim 6$ M$_\odot$ may, however, be consistent with the radio limits so long that the mass transfer from the companion to the WD is very conservative.

(4) Maguire et al. (2013) obtained Very Large Telescope (VLT) XShooter spectra of SN 2012cg -0.8 and $+27.3$ days after $t_{B\rm max}$. They detected blueshifted NaI D absorption that was taken to be tentative evidence for previous mass loss from an SD progenitor. However, Maguire et al. (2013) note that recent DD models (e.g., Shen et al. 2013; Raskin & Kasen 2013) can also reproduce their observations.

(5) Maguire et al. (2016) use VLT spectra from XShooter and FORS2 acquired ~ 340 days after $t_{B\rm max}$ to constrain late-time Hα flux from SN 2012cg. Using scaled models from Mattila et al. (2005), Maguire et al. (2016) placed a strong limit

of < 0.005 M$_\odot$ on the amount of solar-metallicity material present at low velocity, $\lesssim 1000$ km s^{-1}, in SN 2012cg. This limit strongly disfavors a hydrogen-rich SD companion in the progenitor system of SN 2012cg (Maguire et al. 2016). Additionally, Maguire et al. (2016) find no evidence for low velocity, $\lesssim 1000$ km s^{-1}, He$_{\rm I}$ emission at 5876, 10830, and 20590 Å in their XShooter visible and near-IR (NIR) spectra. However, no theoretical model predictions of the peak luminosity for these He features exist and it is not clear if these observations rule out material removed from a He star companion.

(6) Graur & Maoz (2012) used archival HST preexplosion *WFPC*2 images of NGC 4424 to obtain magnitude limits on the progenitor system of $F606W > 25.5$ and $F814W > 25.8$ mag. These limits rule out most supergiants as a possible binary companion.

(7) Graur et al. (2016) observed SN 2012cg to very late times with HST and claim their observations are better described by the nuclear synthetic yields expected from the SD channel. However, these observations are in a single long-pass filter making the measured decay sensitive to changes in the underlying spectral energy distribution. Graur et al. (2016) also note that their observations are consistent with a light echo.

(8) Liu & Stancliffe (2016) attempted to reconcile these observational studies with theoretical predictions from binary evolution and population-synthesis calculations for a range of progenitor scenarios. They find that either a SD progenitor with a 6 M$_\odot$ MS companion or a DD model with carbon-oxygen WD donor might be the progenitor of SN 2012cg, but both scenarios are in conflict with at least some of the reported observations. The most difficult observations to reconcile are the early-time light-curve detection from Marion et al. (2016) and the late-time hydrogen limits from Maguire et al. (2016).

In this study, we add a new late-time Hα constraint, a new X-ray constraint, and reanalyze a timely prediscovery photometric observation of SN 2012cg. Our findings agree with the Maguire et al. (2016) Hα limits and disagree with the Marion et al. (2016) claim of an excess in the early-time light curve from SN 2012cg. When our constraints are considered with other studies of SN 2012cg's progenitor system, the available observations strongly favor a DD progenitor. In Section 2, we present our new deep nebular phase spectra and place a limit on the amount of hydrogen-rich, low-velocity material possible in SN 2012cg. In Section 3, we describe and discuss *Swift* X-ray observations and limits. In Section 4, we present the MASTER photometry, refit the early-time light curve, and place constraints on the presence of a non-degenerate companion. Finally, in Section 5, we discuss the observational constraints on SN 2012cg and conclude that a DD model is the most likely progenitor of SN 2012cg.

Throughout this paper we assume total reddening of SN 2012cg of $E(B-V) = 0.15$ and a ratio of total to selective absorption $R_V = 2.6$ (Amanullah et al. 2015).

2. THE SEARCH FOR COMPANION MATERIAL

In this section, we place a deep and constraining limit on the presence of hydrogen-rich, low-velocity material in SN 2012cg. In Section 2.1, we describe our Large Binocular Telescope (LBT) + Multi-Object Double Spectrographs (MODS; Pogge et al. 2010) nebular-phase observations and their reduction. In Section 2.2, we place a limit on the Hα flux present in our spectrum. In Section 2.3, we use the models of Mattila et al. (2005) to translate this Hα flux into a limit on the presence of low-velocity, hydrogen-rich material and

---

[9] Only SN 2011fe and SN 2014J have deeper limits in the radio.

compare to the previously published limits of Maguire et al. (2016).

2.1. *LBT+MODS Observations*

We obtained a high-signal-to-noise spectrum of SN 2012cg 286 days after $t_{B\mathrm{max}}$ (MJD = 56368.3) using LBT/MODS. We obtained 8×1200s exposures through a $1''$ wide slit. To perform basic CCD reductions on our spectrum, we followed the *MODS Basic CCD Reduction with modsCCDRed* manual[10]. We then performed cosmic ray rejection using L.A. Cosmic (van Dokkum 2001) and combined each channel's 2-D spectra for each epoch. The sky subtraction and one-dimensional extraction were performed with the modsIDL pipeline.[11] We did not attempt to correct small-scale telluric absorption bands. This will not adversely affect our results because the telluric absorption occurs on wavelength scales smaller than the Hα emission expected from the SN and there are no strong telluric features around Hα at the redshift of NGC 4424. Also, we avoid adding additional noise from telluric spectra to our SN spectrum.

We acquired the SN 2012cg spectrum under nonphotometric conditions with a relatively narrow ($1''$) slit, so it is necessary to scale the fluxes of our spectrum to place them on an absolute flux scale. To do this, we performed aperture photometry on our Sloan r (Fukugita et al. 1996) acquisition images using the IRAF package *apphot*. We used the seven bright stars in the image to put our photometry on the Sloan Digital Sky Survey (SDSS; York et al. 2000) Data Release 7 (Abazajian et al. 2009) magnitude system. We determined the SN was $r \sim 19.7$ mag. We then scaled the spectrum so that its synthetic r-band photometry matched the computed r-band aperture photometry. From Shappee et al. (2013b), we estimate that our absolute flux calibration in the R band (where Hα is located) is accurate to 10% or better.

2.2. *Hα Flux limit*

We followed the methods presented in Leonard (2007) to place Hα limits on the spectrum of SN 2012cg. First, we determined a continuum by smoothing the spectrum with a second-order Savitsky-Golay smoothing polynomial (Press et al. 1992) with a width of 250 Å. This width is significantly larger than the expected velocity width of any Hα feature. Our nebular phase spectrum and continuum fit in the vicinity of Hα are shown in the top panel of Figure 1 binned to their approximate spectral resolution. Second, we removed this continuum, as shown in the bottom panel of Figure 1. Last, we examined the residuals for narrow Hα emission. We searched for Hα emission within ± 1000 km s^{-1} (± 22 Å) about Hα at the redshift of NGC 4424. There is no evidence for any Hα emission in the spectrum.

Following Leonard & Filippenko (2001) and Leonard (2007), we compute a 3σ upper bound on the equivalent width as:

$$W_\lambda(3\sigma) = 3\Delta\lambda \,\Delta I \sqrt{W_{\mathrm{line}}/\Delta\lambda} \,\sqrt{1/B}$$
$$= 3\Delta I \sqrt{W_{\mathrm{line}} \,\Delta X}, \tag{1}$$

where $\Delta\lambda$ is the width of a resolution element (in Å); ΔI is the 1σ root-mean-square fluctuation of the flux around a normalized continuum level; W_{line} is the full-width at half-maximum
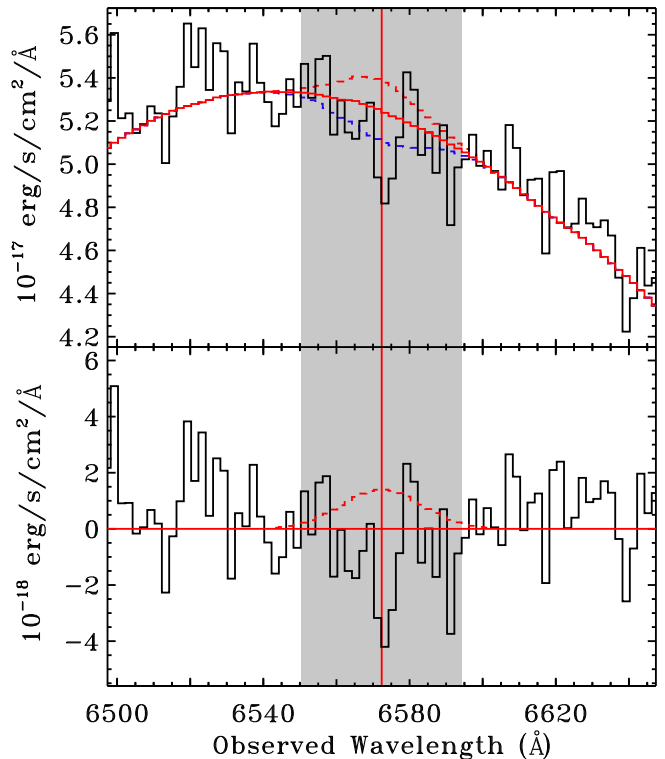
FIG. 1.— Nebular phase spectrum of SN 2012cg, illustrating our Hα flux limit of 3.28×10^{-17} erg s^{-1} cm^{-2}. The rest wavelength of Hα is indicated by the vertical red line, and the gray shaded region shows where hydrogen emission would be expected (± 1000 km s^{-1} = ± 22 Å about Hα). Adopting the models of Mattila et al. (2005), these limits translate into a $\lesssim 7.8 \times 10^{-3}$ M$_\odot$ limit on the amount of solar-abundance material stripped from the companion. Note that a weak, narrow Hα absorption line, likely from the host galaxy, might be present in the spectrum. *Top panel:* The SN spectrum binned to the approximate spectral resolution (2.0 Å; black solid); smoothed continuum (solid red); smoothed continuum with Hα limit added (dashed red); and smoothed continuum with the Hα limit subtracted (dashed blue) are shown. *Bottom panel:* SN spectrum with smoothed continuum subtracted (solid black) as compared to the Hα limit (dashed red) are shown. A horizontal solid red line at zero is shown for reference.

(FWHM) of the expected spectral feature (in Å); B is the number of bins per resolution element in the spectrum; and ΔX is the bin size of the spectrum (in Å). For the spectrum shown in in Figure 1, $\Delta I = 0.031$ Å and $\Delta X = 4$ Å, leading to $W_\lambda(3\sigma) = 0.63$ Å for $W_{\mathrm{line}} = 22$ Å.

2.3. *The Search for Hα*

To translate this equivalent width limit into a constraint on the amount of material stripped from a non-degenerate companion, we follow the analysis of Mattila et al. (2005). Mattila et al. (2005) estimate that 0.05 M$_\odot$ of solar-abundance material 380 days after explosion produces an Hα feature with a peak luminosity of $\sim 3.36 \times 10^{35}$ ergs s^{-1} Å^{-1}. Accounting for the distance to NGC 4424 and the measured extinction of SN 2012cg, the expected Hα peak flux from 0.05 M$_\odot$ of stripped material in SN 2012cg is 9.0×10^{-18} erg s^{-1} cm^{-2} Å^{-1}. If we assume the line is a Gaussian with FWHM 22 Å, then this feature would have an equivalent width of $W_\lambda(0.05 \text{ M}_\odot) = 4.0$ Å. Scaling linearly from the equivalent width of the Hα emission line to the amount of stripped material, we place an upper limit on the amount of solar-abundance material in SN 2012cg of 7.8×10^{-3} M$_\odot$.

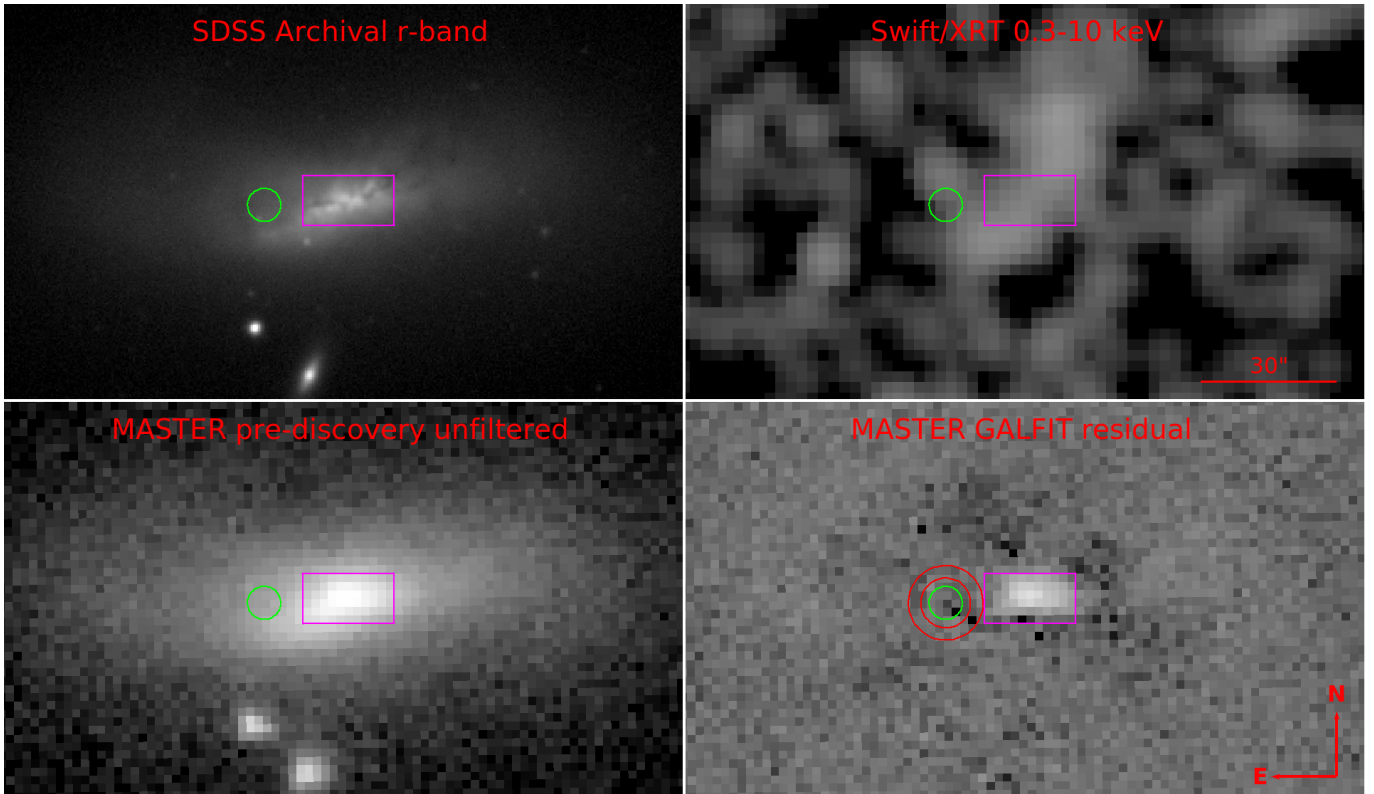This limit agrees with the < 0.005 M$_\odot$ limit reported by

FIG. 2.— Optical and X-ray images at the location of SN 2012cg. *Top left panel:* SDSS *r*-band preexplosion image. *Top right panel: Swift*/XRT 0.3-10 keV X-ray image. *Bottom left panel:* MASTER prediscovery unfiltered image. *Bottom right panel:* GALFIT residual image of MASTER prediscovery unfiltered image. The green circles and the red annulus indicate the aperture and sky region, respectively, used for the MASTER's photometry, centered on the SN position. The purple rectangle shows the masked central region used in the GALFIT fit.

Maguire et al. (2016), who also scale from the Mattila et al. (2005) 380-day model. However, because our observation was acquired earlier (286 vs. ~ 340 days after $t_{B\text{max}}$), when a given mass of material is expected to be more luminous, we view our limit as even more conservative.

3. SWIFT X-RAY LIMITS

In this section, we analyze *Swift* X-ray data obtained for SN 2012cg and place limits on the mass-loss rate and wind velocity from its progenitor system. X-ray emission in a young SN originates from the SN shock interaction with the circumstellar medium (CSM). It directly depends on both the properties of the SN explosion (i.e. shock velocity, ejecta mass) *and* the properties of the environment (i.e. the amount of mass previously ejected by the stellar progenitor). Depending on these properties, different emission processes are expected to contribute to the observed X-rays, in particular: (i) Inverse Compton (IC) scattering of photospheric optical photons off of relativistic electrons accelerated by the SN shock, (ii) synchrotron emission from the same population of accelerated electrons, and (iii) thermal bremsstrahlung. In the low-density regime expected around Type Ia SN progenitors, IC emission has been shown to dominate the X-ray emission at $t \lesssim 40$ days (see Chevalier & Fransson 2006 for a review). In Section 3.1 we describe the *Swift* observations, and we constrain the 0.3-10 keV X-ray flux. In Section 3.2, we place limits on SN 2012cg's progenitor system mass-loss rate.

3.1. *Swift-XRT Observations*

The X-Ray Telescope (XRT, Burrows et al. 2005) on board the *Swift* satellite (Gehrels et al. 2004) started observing

SN 2012cg on 2012 May 18 UTC (*MJD* = 56065.8) and carried out an extensive follow-up campaign. Here we concentrate on observations obtained within ~ 30 days of explosion (*MJD* $\leq$ 56088.2), which offer the best opportunity to constrain the presence of X-ray radiation originating from IC emission. The XRT data were analyzed using HEASOFT (v6.15) and corresponding calibration files. We used standard filtering and screening criteria.

Combining the 24.7 ks of *Swift*/XRT data collected in this time interval, we find no evidence for X-ray emission from a point source at the position of SN 2012cg, with a 3σ count-rate limit of 1.1×10^{-3} c/s (0.3-10 keV). Unfortunately, unresolved diffuse X-ray emission from the host galaxy prevents us from obtaining a deeper limit. Figure 2 shows the *Swift*/XRT 0.3-10 keV X-ray image. The Galactic neutral hydrogen column density in the direction of SN 2012cg is $N(H)_{MW} = 1.5 \times 10^{20}$ cm^{-2} (Kalberla et al. 2005). From the measured total reddening and assuming a Galactic dust-to-gas ratio, we infer an intrinsic $N(H)_{int} \sim 5.5 \times 10^{20}$ cm^{-2}. With these parameters and adopting an absorbed power-law spectral model with photon index $\Gamma = 2$, the count-rate limit above translates into an unabsorbed flux limit $F < 5.1 \times 10^{-14}$ erg s^{-1}cm^{-2}, corresponding to $L < 1.4 \times 10^{39}$ erg s^{-1} (0.3-10 keV).

3.2. *Constraints on the progenitor system mass-loss rate from X-ray observations*

To place constraints on the progenitor-system mass-loss rate, we adopted the generalized IC formalism developed in Margutti et al. (2012). We assumed the following: 1) the SN outer density structure is $\rho_{SN} \propto R^{-n}$ with $n \sim 10$ (Matzner
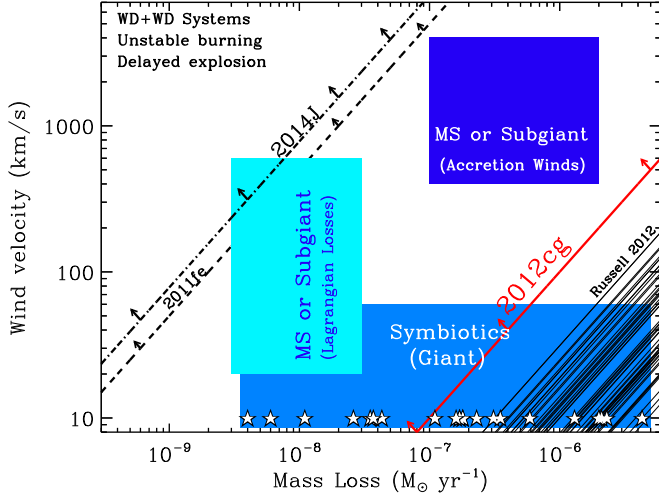
FIG. 3.— Limits on mass loss rates as a function of wind velocity. The limit for SN 2012cg from the *Swift*/XRT flux limits are shown by the solid red line. For comparison, limits on SN 2012cg's progenitor system mass-loss rate from *Swift*/XRT X-ray non-detections are shown. The limits from SN 2011fe (Margutti et al. 2012) and SN 2014J (Margutti et al. 2014) are represented by the dashed and dot-dashed lines, respectively. Other *Swift* limits are indicated by lines in the lower right of the figure (Russell & Immler 2012). Regions for possible SNe Ia progenitor systems are also indicated. White stars indicate the measured mass loss rates of Galactic symbiotic systems for an assumed $v_w = 10 \, \mathrm{km \, s^{-1}}$

& McKee 1999), 2) the electrons are accelerated by the SN shock in a power-law distribution $n(\gamma) \propto \gamma^{-p}$ with $p = 3$, as found from radio observations of hydrogen-stripped SN explosions (e.g. Soderberg et al. 2006), and 3) the fraction of post-shock energy density in relativistic electrons is $\epsilon_e = 0.1$ where the limit on the density scales as $(\epsilon_e/0.1)^{-2}$. (See Appendix A in Margutti et al. 2012.)

We next estimated the bolometric luminosity of SN 2012cg, which is required to translate the X-ray flux limit into a physical limit on mass loss in the progenitor system. We used the UV through NIR photometry published by Marion et al. (2016). For each epoch, we corrected for the observed extinction and distance to NGC 4424 and then integrated the flux density over the wavelength range of the observations. We lack NIR measurements after 9 days past $t_{B\max}$, so we linearly extrapolated the NIR photometry and added a conservative error estimate. For a 10,000 K blackbody, the amount of flux falling outside the wavelength range covered by the photometry is $\sim 7\%$. We adopt this correction to reconstruct the bolometric luminosity of SN 2012cg around the time of the optical peak.

By combining the bolometric light curve with the X-ray limits calculated in Section 3.1, we can constrain the environment density around SN 2012cg. For an ISM medium where $\rho_{\rm CSM} = const$, we derive $\rho_{\rm CSM} < 10^5 \, \mathrm{cm^{-3}}$. However, a star that has been losing material at constant rate $\dot{M}$ gives rise to a wind-like CSM where $\rho_{\rm CSM} = \dot{M}/(4\pi r^2 v_w)$, where v_w is the wind velocity. For a wind-like medium, we infer $\dot{M} < 10^{-6} \, \mathrm{M_\odot \, yr^{-1}}$ for $v_w = 100 \, \mathrm{km \, s^{-1}}$.

In Figure 3, we compare these limits to published limits (Margutti et al. 2012, 2014; Russell & Immler 2012) and candidate SNe Ia progenitor systems. We find that, because of the X-ray emission from the host galaxy, our *Swift*/XRT limits are not very constraining. We can rule out only a fraction of symbiotic progenitor systems, and we would not expect to detect signatures from MS or subgiant companions.

4. EARLY-TIME LIGHT CURVE AND COMPANION CONSTRAINTS

If the progenitor of an SN Ia is a WD accreting from a non-degenerate companion, then the SN ejecta will interact with the companion and potentially produce an observable feature in the rising light curve at early times. Such a signature is dependent on the viewing angle, with the strongest effect occurring when the companion lies along the line of sight between the observer and the SN. At a fixed viewing angle, this emission scales proportionally with R_c.

In this section, we constrain the radius of a possible companion in the progenitor system of SN 2012cg using its very early-time light curve. In Section 4.1, we introduce light curves from Marion et al. (2016). In Section 4.2 we present three prediscovery observations that were not included in the analysis of Marion et al. (2016). In Section 4.3, we closely follow the methods of Shappee et al. (2016b) to fit the early-time light curves and constrain the time of first light ($t_{\rm first}$). Finally, in Section 4.4, we use these observations, our estimate of $t_{\rm first}$, and the interaction models of Kasen (2010) to place stringent limits on R_c.

4.1. *KAIT, LCOGT, FLWO, Swift, and ROTSE Observations*

We use the optical photometry published by Marion et al. (2016) from KAIT (*B*, *V*, *R*, and *I*), FLWO (*U*, *B*, *V*, *r*, and *i*), LCOGT (*B* and *V*), ROTSE-IIIb (unfiltered but calibrated to *r*-band), and the UV/Optical Telescope (UVOT; Roming et al. 2005) on board *Swift* (*u*, *b*, and *v*). The NIR observations from the Peters Automated Infrared Imaging Telescope presented in Marion et al. (2016) were not acquired early enough to be useful for fitting $t_{\rm first}$ or constraining a possible companion, and they are not used in this section. Additionally, there were only 2, 2, and 3 *Swift* UV observations in the *uvw2*, *uvm2*, and *uvw1* filters within 6 days of discovery, respectively[12], so these observations are also not useful for constraining $t_{\rm first}$ but are discussed in Section 5.

We transformed the *Swift* b and v observations to Bessel *B* and *V* bands, respectively, using the UVOT-Johnson *UBV* color corrections[13] derived from the Pickles stars. These transformations are small, < 0.03 mag, and do not qualitatively affect our results. We transformed the *Swift* u into AB-magnitudes using the transformations presented on the *Swift* website[14] and, compare it directly Sloan *u* data because the filter response functions are similar. The *Swift* u observations do not qualitatively affect our $t_{\rm first}$ fits and are not used to constrain R_c, but we include them as a comparison for the ground-based *u*-band photometry.

4.2. *Prediscovery Observations*

There have been three prediscovery observations reported in the literature:
(1) The previous KAIT observation of the host galaxy of SN 2012cg was on 2012 May 12.3 UTC ($MJD = 56059.3$), 4.9 days before discovery (Silverman et al. 2012).
(2) Cortini et al. (2012) report a 19.0 magnitude unfiltered upper limit using a Celestron C14 telescope + Starlight X-Press SXVR H9 camera on 2012 May 14.9 UTC ($MJD = 56061.9$), 2.6 days before discovery. The Starlight X-Press SXVR H9

---

[12] We note that only two of the first three *uvw1* observations are shown in Figure 5 of Marion et al. (2016).
[13] http://heasarc.gsfc.nasa.gov/docs/heasarc/caldb/swift/docs/uvot/uvot_caldb_coltrans_02b.pdf
[14] http://swift.gsfc.nasa.gov/analysis/uvot_digest/zeropts.html

camera's efficiency peaks at 5400Å[15], and Silverman et al. (2012) report this limit as R band. Calibrating an unfiltered observation to a red filter is a conservative when placing constraints on a possible shock interaction because the interaction is expected to be stronger at shorter wavelengths.
(3) As part of the ongoing MASTER survey (Lipunov et al. 2010), we acquired an unfiltered prediscovery image on 2012 May 15.79 UTC ($MJD = 56062.79$), 1.43 days before discovery. Lipunov & Krushinsky (2012) report a marginal detection of SN 2012cg at $R \approx 19$ mag in this image.

In an attempt to verify the prediscovery MASTER detection, we reanalyze this prediscovery image. Typically, we would use image subtraction to remove the host galaxy light with images taken at the same location and instrument without the SN present. However, no additional images are available without SN 2012cg being present. Instead, we used GALFIT (Peng et al. 2002) to model the large-scale, 2-D light distribution of the galaxy. A nearby star served as a PSF model for the Sersic fit. Neighboring objects were also modeled and simultaneously fit, with initial guesses for the Sersic parameters obtained from SExtractor. The complex structure of the host galaxy warranted two Sersic components, especially given the large residuals from a single-component fit. Indeed, both components provided extended fits to the galaxy light distribution. Additionally, we masked the central region so that the fit would be driven by the smooth extended light at large radii around the SN. Figure 2 presents the SDSS archival r-band image, the MASTER prediscovery image, and the GALFIT residual image.

We then performed aperture photometry at the location of SN 2012cg using the IRAF *apphot* package and calibrated the results to r-band. Again, calibrating an unfiltered magnitude to a red filter is a conservative choice. There was no excess flux detected at the location of SN 2012cg, and we place a 3-sigma limit of $r > 19.7$ mag. We note that the SDSS r-band image reveals a point source near the location of SN 2012cg. To verify that this source has not substantially affected our limit, we performed aperture photometry on the SDSS r-band image and found that this source has $r = 20.3 \pm 0.6$, which is significantly fainter than our upper limit. Finally, to verify that any flux from the SN is not impacting the GALFIT fit, we injected artificial sources at the location of the SN in the reduced image, ran GALFIT on the resulting image, and then attempted to recover the source. When injecting 18.5, 19.0 and 19.5 mag sources, we recover each source at 18.80 ± 0.19, 19.12 ± 0.24, and 19.41 ± 0.28 mag, respectively. These artificial source tests show that our method effectively removes the galaxy light while not significantly affecting the flux from point sources.

4.3. *Early-Time Light Curve Fit*

To determine t_{first}, we followed the methods presented in Shappee et al. (2016b). We modeled each band's photometry as an independent power law with index (α_i) but forced all bands to have the same t_{first}. We used the emcee package (Foreman-Mackey et al. 2013), a Python-based implementation of the affine-invariant ensemble sampler for Markov chain Monte Carlo (MCMC), to perform the fit to each light curve. As is done in Goobar et al. (2015) and Shappee et al. (2016b), we fit the data in flux space (not logrithmic magnitudes) to allow the natural treatment of non-detections. We

TABLE 1
FIT LIGHT CURVE
PARAMETERS

band	α
u	$3.30^{+0.36}_{-0.38}$
B	$2.41^{+0.19}_{-0.22}$
V	$2.25^{+0.22}_{-0.18}$
r	$2.19^{+0.20}_{-0.16}$
R	$2.53^{+0.33}_{-0.32}$
$clear$	$1.89^{+0.56}_{-0.73}$
i	$2.16^{+0.20}_{-0.15}$
I	$2.21^{+0.18}_{-0.15}$

fit all observations obtained within 6.5 days of discovery, but the resulting fits were statistically unsatisfactory, at least partially because the photometry reported in Marion et al. (2016) had underestimated errors. We then scaled the errors for each filter so that χ^2 per degree of freedom was 1. We then refit all the observations obtained within 6.5 days of discovery. The best-fit power laws for each filter and their corresponding 1-sigma uncertainties are shown in Figure 4. We find that JD $t_{\mathrm{first}} = 2456062.30^{+0.24}_{-0.26}$, implying that SN 2012cg was discovered $2.42^{+0.24}_{-0.26}$ days after t_{first} and that $t_{\mathrm{rise}} = t_{B\mathrm{max}} - t_{\mathrm{first}} = 19.50^{+0.56}_{-0.56}$ days. The best-fit α parameters for each band are presented in Table 1. We note that the original fit (before scaling errors) is contained within our reported parameter ranges.

To estimate the systematic errors in our estimate of t_{first}, we varied the data range and repeated our MCMC fit to the light curves. The resulting t_{first} and 90% confidence intervals when fitting various data ranges are shown in Figure 5. To be conservative, we adopt the range -2.9 to -1.8 days from discovery for t_{first} when placing progenitor constraints.

4.4. *Progenitor System Constraints*

To place constraints on the progenitor system of SN 2012cg, we first create absolute-magnitude light curves. As elsewhere in the manuscript, we assume a total reddening of $E(B-V) = 0.15$ (Amanullah et al. 2015), a ratio of total-to-selective absorption $R_V = 2.6$, and a distance of 15.2 ± 1.9 Mpc ($\mu = 30.90 \pm 0.3$ mag). We add the distance modulus errors in quadrature with the photometric errors.

We constrain the radius of a possible non-degenerate companion by using the analytic models provided by Kasen (2010). We note that this is conservative because we are ignoring light from the SN itself and attributing all flux to an interaction with a companion. Because the time of explosion (t_{exp}) is uncertain, we explore a variety of t_{exp} and their corresponding constraints on R_{c}. The general procedure is to choose an t_{exp} and then find the maximum R_{c} that is consistent with the early-time data, assuming the secondary filled its Roche lobe. This introduces a weak dependence on the mass ratio of the binary, and we simply assume the primary and companion masses of 1.4 and 1 $M_{\odot}$, respectively. The results are summarized in Figure 6, which shows that $R_{\mathrm{c}} < 0.18 R_{\odot}$ if t_{exp} is within our conservative estimate of t_{first}. While t_{exp} and t_{first} have sometimes been used interchangeably in the literature, differences arise because of a possible dark phase between the explosion and when the SN first starts to brighten (Hachinger et al. 2013; Piro & Nakar 2014; Piro & Morozova 2016). If SN 2012cg did have a dark phase, than t_{exp} might be earlier than our conservative estimate of t_{first}. If t_{exp} was 3.5 days before discovery, our limit weakens but still constrains
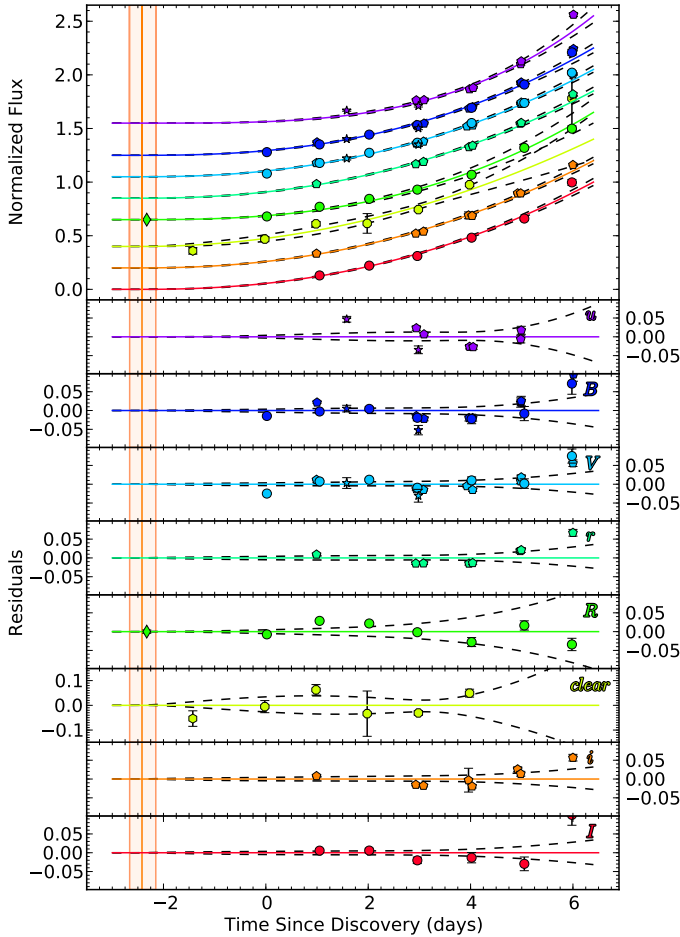
FIG. 4.— Early-time light curves of SN 2012cg with power-law fits to observations obtained within 6.5 days of discovery. Observations from KAIT (circles), FLWO (pentagons), LCOGT (squares), *Swift* (stars), MASTER (hexagon), ROTSE-IIIb (octagons), and Cortini et al. (2012) (diamond) are shown with filled symbols. Unscaled error bars (see Section 4.3) are shown but are sometimes smaller than the points. Colored solid lines are the best-fit power laws while dashed black lines show each fit's 1-sigma range. The vertical orange line shows the best-fit t_{first} and its uncertainty (see Section 4.3). **Top panel:** Light curves normalized by their flux at 5 days after discovery with an added constant. **Bottom panels:** Residuals from the best-fit power laws for each individual filter.
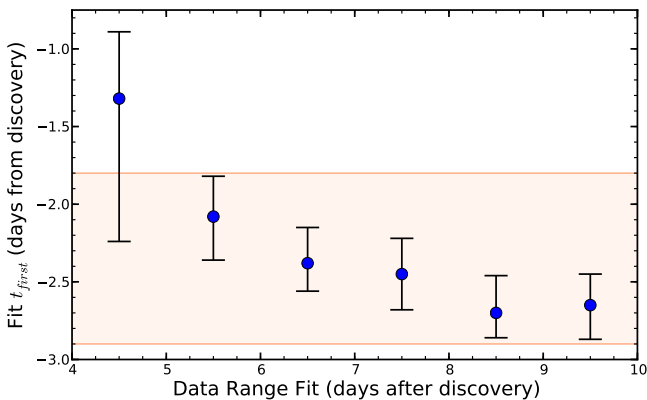
FIG. 5.— Estimates of t_{first} as a function of the data range fit and their 90% confidence intervals. The orange region shows the conservative estimate for t_{first} we adopt to place constraints on the progenitor system (see Section 4.4).
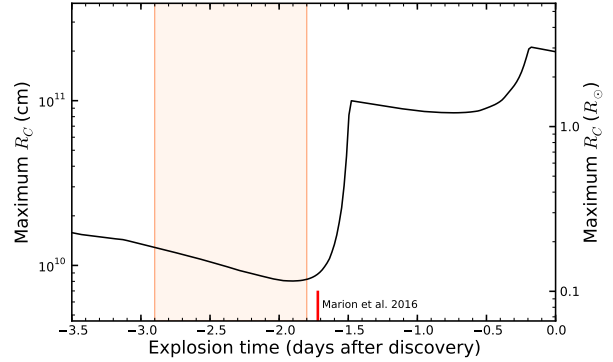
FIG. 6.— Maximum allowed companion radius as a function of explosion time assuming Roche-lobe overflow and a 1 $M_\odot$ companion. The orange region shows the conservative estimate for t_{first} we adopt (see Section 4.4). The red tick mark shows the t_{first} fit by Marion et al. (2016). The constraint on R_c uses our MASTER upper limit, which was not part of the Marion et al. (2016) analysis.

$R_c < 0.23$ $R_\odot$. These estimates assume a viewing angle of 15 degrees.

Although there are a broad range of potential progenitor scenarios, non-degenerate companions can roughly be broken into roughly three main classes: 1) red giant companions with $R_c > 100 R_\odot$ that are similar to the observed binaries RS Oph and T CrB (e.g., Hachisu & Kato 2001), 2) helium star companions with $R_c \sim 0.3 - 6 R_\odot$ that are like the helium-nova system V445 Pup (e.g., Kato et al. 2008), or 3) main-sequence or subgiant companions with $R_c \sim 0.4 - 4 R_\odot$ that are similar to U Sco (e.g., Thoroughgood et al. 2001). Our limits on R_c rule all three of these for all but the most unfavorable viewing angles.

5. PROGENITOR OF SN 2012CG

Even though SN 2012cg is one of the best-studied SNe Ia to date, the nature of its progenitor is still being debated as we discussed in the introduction. Specifically, it is difficult to reconcile the claimed early-time light curve detection of a $\sim 6 M_\odot$ main-sequence companion from Marion et al. (2016) with the Maguire et al. (2016) deep, late-time limit (< 0.005 $M_\odot$) on the amount of low-velocity, solar-metallicity material (Liu & Stancliffe 2016). In this study, we add a new late-time Hα constraints, a new X-ray constraint, and a new early-time light curve constraint using a timely prediscovery MASTER observation.

We obtained a high-signal-to-noise spectrum of SN 2012cg 286 days after t_{Bmax} using LBT/MODS. We then used the models of Mattila et al. (2005) to place an upper limit of 7.8×10^{-3} $M_\odot$ on the amount of solar-abundance material in SN 2012cg. This limit agrees with the limit of < 0.005 $M_\odot$ reported by Maguire et al. (2016), although we view our limit as more conservative. Determining the expected late-time Hα emission in SNe Ia spectra requires difficult radiative transfer calculations, and theoretical questions remain. Most important, the excitation of Hα emission by gamma-ray deposition should be modeled as a function of time while varying the amount and velocity profile of stripped material. These issues notwithstanding, Maguire et al. (2016) and our mass limit pose a significant challenge to SD models, firmly ruling out MS and RG companions.

We analyzed *Swift* X-ray data for SN 2012cg and place limits on the mass-loss rate and wind velocity from its progenitor system. Because of X-ray emission from the host galaxy, our *Swift*/XRT limits are not very constraining, with

$L < 1.4 \times 10^{39}$ erg s^{-1} (0.3-10 keV). For a wind-like CSM, this implies that $\dot{M} < 10^{-6}$ M$_\odot$ yr^{-1} for $v_\mathrm{w} = 100$ km s^{-1}. For this limit, only a fraction of symbiotic progenitor systems are excluded, and we would not expect to detect X-ray signatures from MS or subgiant companions.

Finally, we carefully reanalyze a pre-discovery MASTER observation in http://adsabs.harvard.edu/abs/2015Natur.521..332Ocombination with published photometry (Silverman et al. 2012; Marion et al. 2016) to estimate t_first. We then looked for the signature expected from an interaction between the SN ejecta and a possible SD companion. Assuming that t_exp is within our range for t_first of -2.9 to -1.8 days from discovery, we constrain the radius of a companion to be $R_\mathrm{c} < 0.18$ R$_\odot$. If t_exp is earlier than our conservative estimate of t_first, then our limit weakens but still constrains $R_\mathrm{c} < 0.23$ R$_\odot$ when t_exp is 3.5 days before discovery. These estimates assume a viewing angle of 15 degrees and rule out a red giant, a helium star, a main sequence, or a subgiant companion for all but the most unfavorable viewing angles.

Our limits on R_c are in agreement with those presented in Silverman et al. (2012). However, they are in stark contrast with the Marion et al. (2016) claim of a blue early-time excess in the optical light curve consistent with the SN ejecta interacting with a ~ 6 M$_\odot$ main-sequence companion. While there are variations between our analyses, the main differences leading to this discrepancy are:

1) Marion et al. (2016) did not include the MASTER predis-covery observation from Lipunov & Krushinsky (2012). This observation proves to be extremely constraining.

2) In this study, we fit unfiltered observations as a separate "filter". Marion et al. (2016) instead shifted the unfiltered ROTSE light curve to match a t^2 model fit to B-band observations between 10 to 14 days before $t_{B\mathrm{max}}$. However, if the ROTSE light curve rises less steeply than B-band light curve, then using the ROTSE observations shifted to match B at later times would lead to a spurious excess in flux at early times. These "overluminous" ROTSE observations would then appear to support a ~ 6 M$_\odot$ main-sequence companion.

3) Marion et al. (2016) do not include the r, R, i, and I light curves when fitting t_first and searching for a signature of a companion. We use these longer wavelength observations.

4) In this study, instead of assuming a fixed t_exp, we estimate our uncertainty on t_first and then vary t_exp when determining R_c limits. This process allows us to quantify the effects of a possible dark phase.

5) In this study, we do not use the *Swift* UV observations because there are not enough early-time observations to robustly fit the rise. Figure 5 of Marion et al. (2016) shows that there is excess flux in the first two *Swift* UV epochs when compared to a $t^{3.6}$ power law. However, this 3.6 power-law index was derived from the U-band light curve, not the UV light curve. Shappee et al. (2016b) found that $uvw2$ and $uvw1$ follow a significantly shallower power law than u band for ASASSN-14lp. If this is also true for SN 2012cg, then fitting *Swift* UV observations with a steeper power law at later times would naturally cause a spurious excess flux at earlier times.

6) Finally, Marion et al. (2016) find that SN 2012cg rises slowly between the first two *Swift* UV epochs. However, the slope between the first and second *Swift* epochs appears to be inconsistent with the ground-based photometry at optical wavelengths, and this trend increases going to bluer wavelengths (see Figure 4). This might point to a problem with

the first or second epochs of *Swift* observations. We reran the Swift photometry ourselves but found no obvious reason why the UV photometry should be wrong. However, in this study we have shown that the longer-wavelength light curves rule out the Kasen (2010) models for the shock interaction between the SN ejecta and a companion. Thus we are left with three possibilities: i) There is significant diversity in the UV rise of SNe Ia intrinsic to their explosions. ii) Our understanding of the interaction between the SN ejecta and a companion is not complete. iii) We are seeing the interaction between the SN ejecta and nearby material in a different geometry and/or distribution than a companion. Perhaps it is the debris from the WD-WD merger (Piro & Morozova 2016)?

The light curves of SNe Ia within days of explosion are sensitive tools that enable us to constrain the physical conditions present in the progenitor systems of SNe Ia immediately prior to explosion. However, there are multiple physical processes and geometries which potentially imprint themselves on these light curves. Thus, we should be careful not to over-interpret limited data, especially limited in wavelength, as evidence for one physical interpretation.

In summary, we do not detect stripped hydrogen-rich material, and we place firm limits on the radius of a possible companion. When our constraints are combined with other studies of SN 2012cg's progenitor system (e.g., Chomiuk et al. 2012a; Graur & Maoz 2012; Silverman et al. 2012; Maguire et al. 2013; Chomiuk et al. 2016; Graur et al. 2016; Liu & Stancliffe 2016; Maguire et al. 2016), the available observations strongly favor a DD progenitor for SN 2012cg.

In the last 7 years we have seen an explosion of companion constraints from nearby, bright SN that have been observed extremely early: SN 2009ig (< 6 M$_\odot$; Foley et al. 2012), SN 2011fe ($< 0.1 - 0.25$ R$_\odot$; Bloom et al. 2012; Goobar et al. 2015), KSN 2011a (< 2 M$_\odot$; Olling et al. 2015), KSN 2011b (< 2 M$_\odot$; Olling et al. 2015), SN 2012cg ($< 0.18 - 0.23$ R$_\odot$; this paper), SN 2013dy (< 0.35 R$_\odot$; Zheng et al. 2013), SN 2014J ($\lesssim 0.25 - 4$ R$_\odot$; (Goobar et al. 2015; Siverd et al. 2015), ASASSN-14lp (< 0.3411 R$_\odot$; Shappee et al. 2016b), and SN 2015F (< 1.0 R$_\odot$; Im et al. 2015). These discoveries are a testament to large, nearby transient surveys (e.g., ASAS-SN, Shappee et al. 2014; LOSS, Filippenko et al. 2001; PTF, Law et al. 2009). Similar to Bianco et al. (2011), all these observations easily rule out of giant companions for Type Ia Supernovae. Additionally, there are 3 SNe (SN 2011fe, SN 2012cg, SN 2013dy) where the limits rule out main-sequence or subgiant companions and 2 SNe (SN 2011fe, SN 2012cg) where the limits are strong enough to rule out He star companions. And yet, the signatures of an interaction with a sizable companion star have not been unambiguously seen for any normal SN Ia. Assuming the 4 best-constrained SNe are representative of the entire population, the fraction of SNe Ia with $R_\mathrm{c} > 1$ R$_\odot$ is $< 25\%$ is $< 25\%$ with 1-sigma confidence and $< 53\%$ with 2-sigma confidence. We will present a more thorough statistical analysis in a future work.

REFERENCES

Abazajian, K. N., et al. 2009, ApJS, 182, 543
Akerlof, C. W., et al. 2003, PASP, 115, 132
Amanullah, R., et al. 2015, MNRAS, 453, 3300
Antognini, J. M., Shappee, B. J., Thompson, T. A., & Amaro-Seoane, P. 2014, MNRAS, 439, 1079
Bianco, F. B., et al. 2011, ApJ, 741, 20
Bloom, J. S., et al. 2012, ApJ, 744, L17
Brown, P. J., Dawson, K. S., Harris, D. W., Olmstead, M., Milne, P., & Roming, P. W. A. 2012, ApJ, 749, 18
Brown, T. M., et al. 2013, PASP, 125, 1031
Burrows, D. N., et al. 2005, Space Sci. Rev., 120, 165
Cenko, S. B., et al. 2012, The Astronomer's Telegram, 4115, 1
Chevalier, R. A., & Fransson, C. 2006, ApJ, 651, 381
Chomiuk, L., Soderberg, A., Simon, J., & Foley, R. 2012a, The Astronomer's Telegram, 4453, 1
Chomiuk, L., et al. 2012b, ApJ, 750, 164
—. 2016, ApJ, 821, 119
Cortés, J. R., Kenney, J. D. P., & Hardy, E. 2008, ApJ, 683, 78
Cortini, G., et al. 2012, Central Bureau Electronic Telegrams, 3111
Filippenko, A. V., Li, W. D., Treffers, R. R., & Modjaz, M. 2001, in Astronomical Society of the Pacific Conference Series, Vol. 246, IAU Colloq. 183: Small Telescope Astronomy on Global Scales, ed. B. Paczynski, W.-P. Chen, & C. Lemme, 121
Foley, R. J., et al. 2012, ApJ, 744, 38
Foreman-Mackey, D., Hogg, D. W., Lang, D., & Goodman, J. 2013, PASP, 125, 306
Fukugita, M., Ichikawa, T., Gunn, J. E., Doi, M., Shimasaku, K., & Schneider, D. P. 1996, AJ, 111, 1748
Gehrels, N., et al. 2004, ApJ, 611, 1005
Goobar, A., et al. 2015, ApJ, 799, 106
Graur, O., & Maoz, D. 2012, The Astronomer's Telegram, 4226, 1
Graur, O., Zurek, D., Shara, M. M., Riess, A. G., Seitenzahl, I. R., & Rest, A. 2016, ApJ, 819, 31
Hachinger, S., et al. 2013, MNRAS, 429, 2228
Hachisu, I., & Kato, M. 2001, ApJ, 558, 323
Horesh, A., et al. 2012, ApJ, 746, 21
Hoyle, F., & Fowler, W. A. 1960, ApJ, 132, 565
Iben, Jr., I., & Tutukov, A. V. 1984, ApJS, 54, 335
Im, M., Choi, C., Yoon, S.-C., Kim, J.-W., Ehgamberdiev, S. A., Monard, L. A. G., & Sung, H.-I. 2015, ApJS, 221, 22
Johansson, J., Amanullah, R., & Goobar, A. 2013, MNRAS, L59
Kalberla, P. M. W., Burton, W. B., Hartmann, D., Arnal, E. M., Bajaja, E., Morras, R., & Pöppel, W. G. L. 2005, A&A, 440, 775
Kasen, D. 2010, ApJ, 708, 1025
Kasen, D., Röpke, F. K., & Woosley, S. E. 2009, Nature, 460, 869
Kato, M., Hachisu, I., Kiyota, S., & Saio, H. 2008, ApJ, 684, 1366
Katz, B., & Dong, S. 2012, arXiv:astro-ph/1211.4584
Kent, B. R., et al. 2008, AJ, 136, 713
Law, N. M., et al. 2009, PASP, 121, 1395
Leonard, D. C. 2007, ApJ, 670, 1275
Leonard, D. C., & Filippenko, A. V. 2001, PASP, 113, 920

Li, W., et al. 2011, Nature, 480, 348
Lipunov, V., & Krushinsky, V. 2012, The Astronomer's Telegram, 4138
Lipunov, V., et al. 2010, Advances in Astronomy, 2010, 349171
Lipunov, V. M., Panchenko, I. E., & Pruzhinskaya, M. V. 2011, Nature, 16, 250
Liu, Z. W., Pakmor, R., Röpke, F. K., Edelmann, P., Wang, B., Kromer, M., Hillebrandt, W., & Han, Z. W. 2012, A&A, 548, A2
Liu, Z.-W., & Stancliffe, R. J. 2016, MNRAS, 459, 1781
Maguire, K., Taubenberger, S., Sullivan, M., & Mazzali, P. A. 2016, MNRAS, 457, 3254
Maguire, K., et al. 2013, MNRAS, 436, 222
Margutti, R., Parrent, J., Kamble, A., Soderberg, A. M., Foley, R. J., Milisavljevic, D., Drout, M. R., & Kirshner, R. 2014, ApJ, 790, 52
Margutti, R., & Soderberg, A. 2012, The Astronomer's Telegram, 4118
Margutti, R., et al. 2012, ApJ, 751, 134
Marietta, E., Burrows, A., & Fryxell, B. 2000, ApJS, 128, 615
Marion, G. H., et al. 2016, ApJ, 820, 92
Mattila, S., Lundqvist, P., Sollerman, J., Kozma, C., Baron, E., Fransson, C., Leibundgut, B., & Nomoto, K. 2005, A&A, 443, 649
Matzner, C. D., & McKee, C. F. 1999, ApJ, 510, 379
Meng, X., Chen, X., & Han, Z. 2007, PASJ, 59, 835
Munari, U., Henden, A., Belligoli, R., Castellani, F., Cherini, G., Righetti, G. L., & Vagnozzi, A. 2013, NewA, 20, 30
Nomoto, K. 1982, ApJ, 253, 798
Nugent, P., Sullivan, M., Bersier, D., Howell, D. A., Thomas, R., & James, P. 2011, The Astronomer's Telegram, 3581, 1
Olling, R. P., et al. 2015, Nature, 521, 332
Pakmor, R., Kromer, M., Taubenberger, S., Sim, S. A., Röpke, F. K., & Hillebrandt, W. 2012, ApJ, 747, L10
Pakmor, R., Röpke, F. K., Weiss, A., & Hillebrandt, W. 2008, A&A, 489, 943
Pan, K.-C., Ricker, P. M., & Taam, R. E. 2012a, ApJ, 760, 21
—. 2012b, ApJ, 750, 151
Pejcha, O., Antognini, J. M., Shappee, B. J., & Thompson, T. A. 2013, MNRAS, 435, 943
Peng, C. Y., Ho, L. C., Impey, C. D., & Rix, H.-W. 2002, AJ, 124, 266
Piro, A. L., Chang, P., & Weinberg, N. N. 2010, ApJ, 708, 598
Piro, A. L., & Morozova, V. S. 2016, ApJ, 826, 96
Piro, A. L., & Nakar, E. 2014, ApJ, 784, 85
Podsiadlowski, P. 2003, arXiv:astro-ph/0303660
Pogge, R. W., et al. 2010, in Society of Photo-Optical Instrumentation Engineers (SPIE) Conference Series, Vol. 7735, Society of Photo-Optical Instrumentation Engineers (SPIE) Conference Series
Press, W. H., Teukolsky, S. A., Vetterling, W. T., & Flannery, B. P. 1992, Numerical recipes in C. The art of scientific computing, ed. Press, W. H., Teukolsky, S. A., Vetterling, W. T., & Flannery, B. P.
Raskin, C., & Kasen, D. 2013, ApJ, 772, 1
Roming, P. W. A., et al. 2005, Space Sci. Rev., 120, 95
Russell, B. R., & Immler, S. 2012, ApJ, 748, L29
Shappee, B. J., Kochanek, C. S., & Stanek, K. Z. 2013a, ApJ, 765, 150
Shappee, B. J., & Stanek, K. Z. 2011, ApJ, 733, 124

Shappee, B. J., Stanek, K. Z., Kochanek, C. S., & Garnavich, P. M. 2016a, ArXiv e-prints

Shappee, B. J., Stanek, K. Z., Pogge, R. W., & Garnavich, P. M. 2013b, ApJ, 762, L5

Shappee, B. J., & Thompson, T. A. 2013, ApJ, 766, 64

Shappee, B. J., et al. 2016b, ApJ, 826, 144

Shappee, B. J., et al. 2014, ApJ, 788, 48

Shen, K. J., Guillochon, J., & Foley, R. J. 2013, ApJ, 770, L35

Silverman, J. M., et al. 2012, ApJ, 756, L7

Siverd, R. J., Goobar, A., Stassun, K. G., & Pepper, J. 2015, ApJ, 799, 105

Soderberg, A. M., et al. 2006, ApJ, 650, 261

Thompson, T. A. 2011, ApJ, 741, 82

Thoroughgood, T. D., Dhillon, V. S., Littlefair, S. P., Marsh, T. R., & Smith, D. A. 2001, MNRAS, 327, 1323

Tutukov, A. V., & Yungelson, L. R. 1979, Acta Astron., 29, 665

van Dokkum, P. G. 2001, PASP, 113, 1420

Wang, B., & Han, Z. 2012, NewAR, 56, 122

Webbink, R. F. 1984, ApJ, 277, 355

Wheeler, J. C., Lecar, M., & McKee, C. F. 1975, ApJ, 200, 145

Whelan, J., & Iben, Jr., I. 1973, ApJ, 186, 1007

Yamaguchi, H., et al. 2015, ApJ, 801, L31

Yamanaka, M., et al. 2014, ApJ, 782, L35

York, D. G., et al. 2000, AJ, 120, 1579

Zheng, W., et al. 2013, ApJ, 778, L15